Ref. Ares(2026)10081595 - 27/10/2026

D3.4. Pilots lines installation and assembly

PHOTOELECTROCATALYTIC SYSTEMS FOR SOLAR FUELS ENERGY INTEGRATION INTO THE INDUSTRY WITH LOCAL RESOURCES

Grant Agreement Number 101118129

Deliverable name:	D3.4 - Pilots lines installation and assembly
Deliverable number:	3.4
Deliverable type:	Report
Work Package:	WP3: Pilot design and testing activities under industrial environment
Lead beneficiary:	TOR
Contact person:	Carlos Concepcion
Dissemination Level:	Public
Due date for deliverable:	August 30th 2026

Funded by the European Union

Funded by the European Union. Views and opinions expressed are, however, those of the author(s) only and do not necessarily reflect those of the European Union or CINEA. Neither the European Union nor the granting authority can be held responsible for them.

Document control page

Author(s):	Carlos Concepcion
Contributor(s):	Maciej -Gryszel, Ana Varlec, Sabina Žlindra
Reviewer(s):	All
Version number:	4
Contractual delivery date:	30th August 2026
Actual delivery date:	27th October 2026
Status:	Final document

Revision history

Version	Date	Author/Reviewer	Notes
v.0	16-7-2026	Carlos Concepcion	Draft
v.1	7-10-2026	Maciej -Gryszel	Addition
v.2	16-10-2026	Ana Varlec, Sabina Žlindra	Addition
v.3	19-10-2026	Carlos Concepcion	Coordinator revision acceptance
v.4	22-10-2026	Ana Varlec ,Sabina Žlindra	Revision

Acknowledgments

The work described in this publication was subsidised by Horizon Europe (HORIZON) framework through the Grant Agreement Number 101118129.

Disclaimer

Funded by the European Union. Views and opinions expressed are, however, those of the author(s) only and do not necessarily reflect those of the European Union or CINEA. Neither the European Union nor the granting authority can be held responsible for them.

All the contributors to this deliverable declare that they:

- *Are aware that plagiarism and/or literal utilisation (copy) of materials and texts from other projects, works and deliverables must be avoided and may be subject to disciplinary actions against the related partners and/or the Project consortium by the EU.*
- *Confirm that all their individual contributions to this deliverable are genuine and their own work or the work of their teams working in the Project, except where it is explicitly indicated otherwise.*
- *Have followed the required conventions in referencing the thoughts, ideas and texts made outside the Project.*

Table of contents

Executive summary 4

1. INTRODUCTION 5

1.1 Description of the content and WP relation. 6

2. ASSEMBLY OF PILOTS 7

2.1 Pilot architecture and PV-electrochemical integration 7

2.2 Electrochemical cell configuration 8

2.2.1 The electrochemical cell architecture 8

2.2.2 Electrolyte circulation and gas management 13

2.3 Light concentration, thermal integration and tracking 13

2.4 Temperature and electrical monitoring 14

2.5 Expected product generation and product monitoring 14

2.6 Photovoltaic modules and catalyst integration 15

2.7 Adaptations Introduced During Pilot Construction 15

2.10 Equipment images 21

3. INTEGRATION OF PILOTS AT DEMO 33

3.1 Integration of methanol pilot at Torrecid 33

3.2 Integration of Hydrogen pilot at Steklarna 34

4. CONCLUSION 35

Executive summary

The PHOTOSINT project offers solutions to the chemical industry's challenges in incorporating renewable energy into its processes. It aims to develop sustainable methods for producing hydrogen and methanol as energy carriers, using only sunlight, wastewater, and CO_2 as inputs, thus increasing industry self-sufficiency. The approach relies on solar-driven artificial photosynthesis, focusing on creating new catalytic materials that are earth-abundant and refining existing ones to enhance catalytic efficiency. The design of the PEC cell will be optimized to maximize STF (Solar-To-Fuel) efficiency. Additionally, PHOTOSINT will innovatively concentrate and illuminate the semiconductor surface, expanding the light collection area at similar CAPEX, and incorporate a heat exchange system between the semiconductor and electrochemical cell to boost overall energy efficiency and reduce OPEX. Low-cost, advanced perovskite solar PV cells will also be integrated to power the electrocatalytic process.

The project will focus on studying catalysts to harness sunlight energy for industrial use. The best catalysts identified will be incorporated into prototypes. These results will guide the scaling-up process in pilot plants using tandem PEC cells. This progression is critical to evaluate the feasibility of industrial-scale implementation, enhancing the competitiveness of renewable energy technologies and promoting energy independence. Additionally, MeOH and H_2 will be tested in industrial settings with the goal of achieving TRL4 by the project's end.

The purpose of this deliverable is to provide insight into specific equipment developed in PHOTOSINT addressing the production of methanol and hydrogen using photovoltaic energy and industrial waste streams (CO_2 and water) The deliverable describes the prototype setup and assembly, including the main characteristics of the photovoltaic panel configuration, cell configuration and equipment monitoring. The report includes a description of the validation tests performed before shipping, such as leak tests and a brief description of demo sites for implementation.

1. INTRODUCTION

Global energy demand continues to rise due to economic growth and increasing population, leading to a significant reliance on non-renewable fossil fuels that account for approximately 65% of the world's energy consumption (World energy outook 2020, IEA). This dependency results in substantial greenhouse gas emissions, particularly carbon dioxide (CO_2), which contribute to climate change and environmental degradation (Edenhofer, 2015). Transitioning to sustainable energy systems is imperative to mitigate these adverse effects and meet international environmental targets.

Hydrogen (H_2) and methanol (MeOH) have emerged as promising energy carriers and chemical feedstocks due to their high energy density and versatility in various applications, including fuel cells and synthetic fuels (Ball & Weeda, 2015). Photoelectrochemical (PEC) processes offer a sustainable pathway to produce H_2 and MeOH by utilising solar energy to convert CO_2 and water (H_2O) into valuable chemicals, thus closing the carbon loop and reducing net CO_2 emissions (Bard & Fox, 1995). However, the efficiency and economic viability of PEC processes are currently limited by challenges such as low conversion efficiencies, high operational costs, and material degradation (Lewis & Nocera, 2006). The decarbonisation of Europe's energy-intensive industries increasingly depends on innovative renewable-fuel technologies capable of reducing emissions while strengthening energy security and competitiveness. Within this context, the PHOTOSINT project advances a novel approach based on PEC (photoelectrocatalytic) systems that convert sunlight, wastewater and captured CO_2 into hydrogen and methanol. These solar-driven pathways offer the potential for decentralised, resource-efficient and low-carbon fuel production, complementing existing approaches such as electrolysis and supporting the long-term objectives of the European Green Deal, the EU Hydrogen Strategy and REPowerEU.

The PHOTOSINT project, named PHOTOelectrocatalytic systems for Solar fuels energy INTegration into the industry with local resources, is an initiative granted under the Horizon Europe call HORIZON-CL5-2022-D3-02 and, specifically, topic HORIZON-CL5-2022-D3-02-06: Direct renewable energy integration into process energy demands of the chemical industry. The PHOTOSINT project offers solutions to the chemical industry's challenges in incorporating renewable energy into its processes. It develops sustainable methods for producing hydrogen and methanol as energy carriers, using only sunlight, wastewater, and CO_2 as inputs, thus increasing industry self-sufficiency. The approach relies on solar-driven artificial photosynthesis, focusing on creating new catalytic materials that are earth-abundant and refining existing ones to enhance catalytic efficiency. The design of the PEC cell will be optimized to maximize STF (Solar-To-Fuel) efficiency. Additionally, PHOTOSINT concentrates and illuminates the semiconductor surface, expanding the light collection area at similar CAPEX, and incorporates a heat exchange system between the semiconductor and electrochemical cell to boost overall energy efficiency and reduce OPEX. Low-cost, advanced perovskite solar PV cells will also be integrated to power the electrocatalyst process.

The project focuses on studying catalysts to harness sunlight energy for industrial use. The best catalysts identified will be incorporated into prototypes. These results will guide the scaling-up process in pilot plants using tandem PEC cells. This progression is critical to evaluate the feasibility of industrial-scale implementation, enhancing the competitiveness of renewable energy technologies and promoting energy independence. This document aims to describe the integration and assembly of PEC PHOTOSINT systems for methanol and hydrogen production.

1.1 Description of the content and WP relation.

This deliverable refers to work carried out in Task 3.4. The document describes the overall integration approach, the design and assembly of pilots, starting from equipment supplied by partners. Project partners contribute with the specific components in line with their expertise: CSIC is responsible for the supply of the photovoltaic (PV),cells SU provides the catalysts for methanol production, ICIQ supplies the oxygen evolution reaction (OER) catalysts, and NIC delivers the hydrogen evolution (HER) catalysts. The activities within this Task therefore focus on bringing together these components into a coherent system design, ensuring their compatibility and readiness for integration. This Task provides the technical basis for deployment at demo sites of PEC PHOTOSINT systems for methanol and hydrogen production.

Deliverable 3.4 summarizes results from Task 3.4 in WP3. Work carried out started from Task 3.3, in which different parts of the system were developed.

In the framework of PHOTOSINT, two demos will validate the cell configuration: on the one hand, Steklarna (STE), in which a hydrogen production demo will be installed and on the other, Torrecid (TOR), in which methanol production using CO_2 from the process will be installed. Specific details of equipment were given in D3.3.

The present report covers:

i. Prototypes set up and assembly

ii. Photovoltaic panel configuration.

iii. Cell configuration.

iv. Equipment monitoring.

v. Validation test performed before shipping.

vi. Health and safety guidelines at demo sites.

vii. Description of demo sites for implementation.

2. ASSEMBLY OF PILOTS

Present deliverable starts from Deliverable D3.3, that established the overall integration strategy for the two PHOTOSINT pilot systems and translated the component-level developments of the preceding tasks into an implementable system architecture. Deliverable starts components designed and manufactured by ICIQ, SU, CSIC, NIC and RDM.

Due to material performance constraints regarding aging and transport, it was finally agreed to exclude the photovoltaic panels from the ready-to-ship assembly and install them on site. The catalyst will also be added on site. Within this framework, Task 3.4 has successfully carried out the integration and assembly of the pilots

The two systems considered were Pilot #1 for electrochemical CO_2 conversion to methanol (MeOH) and Pilot #2 for hydrogen evolution (HER). The work carried out in Task 3.4 aimed to integrate the photovoltaic modules, electrochemical cells, flow-management components, light-concentration system, solar tracker, instrumentation, and product-monitoring equipment into complete outdoor pilot installations.

The concept is based on direct PV-to-electrolyser coupling without intermediate power electronics, one PV module per electrochemical cell, series connection of the EC cells and parallel connection of their associated PV modules, and two panel sizes: 3 × 3 cells for methanol and 4 × 4 cells for hydrogen. The design combined individual Fresnel concentrators with dual-axis tracking, thermally coupled PV/electrochemical units, independent fluid circuits, peristaltic pumping, representative rather than exhaustive temperature/electrical monitoring, and dedicated downstream product-measurement systems. The design was explicitly intended as a practical compromise between electrochemical and photovoltaic performance, component availability, catalyst-production capacity, long-term stability, system complexity, and the requirements of future outdoor operation.

Both prototypes were assembled by RDM according to partners' inputs, considering the similarity in design.

2.1 Pilot architecture and PV-electrochemical integration

Based on the information gathered during the preparation of D3.3, one of the key design decisions concerned the electrical coupling between the photovoltaic and electrochemical subsystems. The initial project concept considered larger panels containing approximately 25 electrochemical cells, with each cell operating as an electrically independent unit powered by its own PV module. During the project, this approach was reconsidered for two principal reasons. First, preparation of the required number of large-area catalytic electrodes proved substantially more demanding than originally anticipated. Second, the electrical characteristics of the perovskite modules available for the pilot were not well matched to a single electrochemical cell. The Solaronix modules considered for pilot implementation provided an open-circuit voltage above 10 V but a relatively low short-circuit current of approximately 80 mA, whereas the electrochemical cells required considerably lower operating voltages, generally below 2-2.5 V.

Instead of introducing DC-DC converters to transform the excess PV voltage into additional current, a direct electrical matching strategy was selected. The basic principle

was to connect several electrochemical cells in series while connecting the corresponding photovoltaic modules in parallel. This allowed the relatively high voltage of the PV modules to be utilized by several EC cells operating in series, while parallel connection of the PV modules increased the current supplied to the EC string. The use of DC-DC converters was thereby avoided, reducing additional system complexity, cost, and conversion losses. Importantly, the original physical concept of one PV module associated with each electrochemical cell was retained, so that the planned thermal coupling and individual light-concentration arrangement were not fundamentally changed.

- For Pilot #1, the operating voltage required for methanol production was assumed to be approximately 2.2-2.5 V per electrochemical cell. Three EC cells were therefore connected in series. The three PV modules corresponding to these cells were connected in parallel, giving a nominal short-circuit current of approximately 240 mA per string. The complete pilot consisted of nine cells arranged as a 3 × 3 panel, comprising three electrically equivalent strings. Each string contained three EC cells connected in series and three PV modules connected in parallel.

- For Pilot #2, the required operating voltage per electrochemical cell was assumed to be below 2 V. Consequently, four EC cells were connected in series, while the corresponding four PV modules were connected in parallel, providing a nominal string current of approximately 320 mA. The hydrogen pilot consisted of 16 cells arranged as a 4 × 4 panel, forming four equivalent strings.

A simplifying assumption used for system sizing was that, under concentrated illumination, the current available to an EC string would be approximately equal to the nominal short-circuit current of one PV module multiplied by the number of PV modules connected in parallel. The actual operating currents are expected to be lower than the short-circuit current and dependent on illumination intensity, PV operating voltage, concentration efficiency, and solar position.

2.2 Electrochemical cell configuration

2.2.1 The electrochemical cell architecture

The electrochemical cell architecture was based on the optimized design previously developed in D3.2. The geometry was kept common to both pilots to simplify panel integration and manufacturing, while the construction materials were adapted to the different chemical environments. The cell had an approximately 15 × 15 cm external footprint and a total mass of approximately 2 kg (for Pilot #1) and 3 kg (for Pilot #2). Sealing relied on O-rings located in machined grooves providing a defined compression limit or mechanical "hard stop", improving reproducibility during repeated assembly.

D3.3 specified titanium as the cathodic plate material for both pilots. For the hydrogen pilot, nickel was selected for the anodic plate and heat exchanger because of its stability under alkaline conditions and comparatively good thermal conductivity. For the methanol pilot, which operates under near-neutral conditions, stainless steel 904L was selected for the anodic plate and titanium for the heat exchanger because of concerns regarding nickel corrosion at lower pH.

The cell consists of a PV module, a heat exchanger plate, a PEEK flow field, front and rear compartment flow fields, GDL/PTL layers, a membrane, PTFE gaskets, O-rings,

PEEK liners, and stainless-steel screws. The flow fields guide fluid through the cell, while the GDL/PTL layers support gas and liquid transport. The membrane separates the two sides and allows ions to pass through. The gaskets and O-rings seal the cell, the PEEK liners provide electrical insulation, and the screws hold the assembly together.

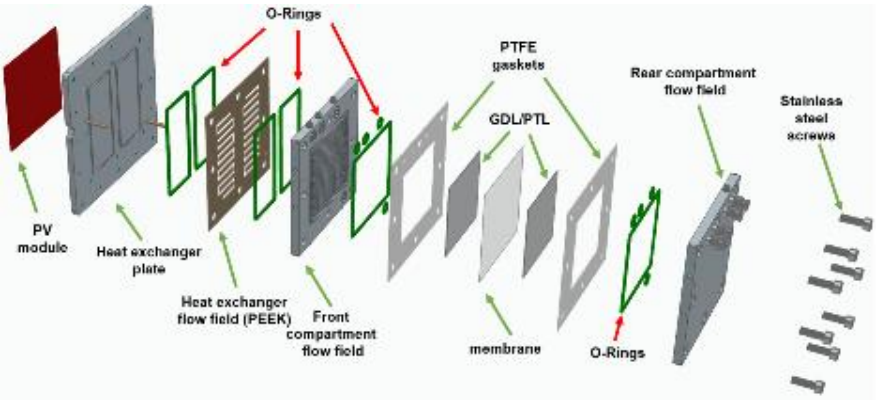
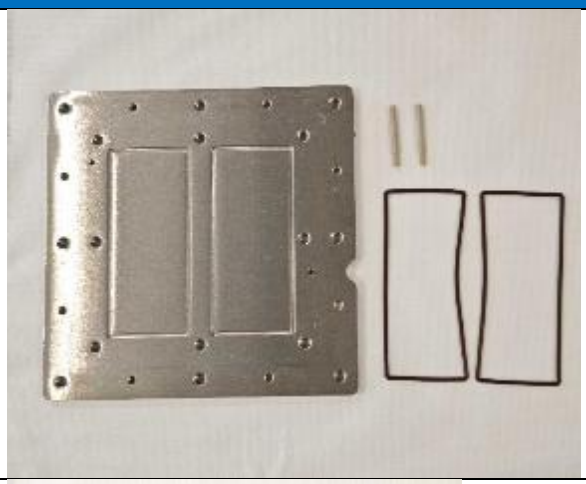
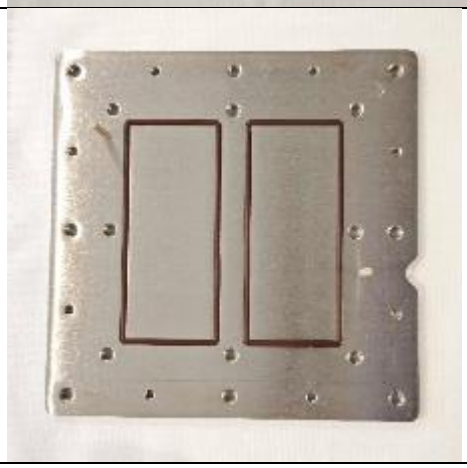
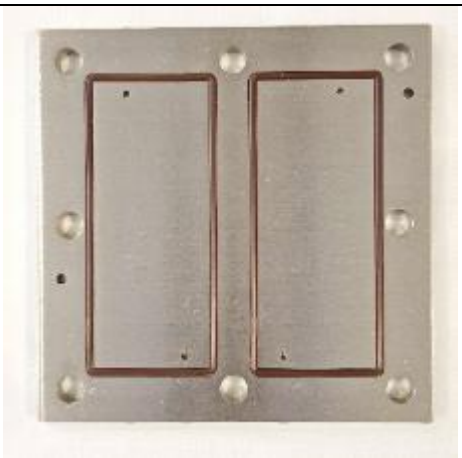
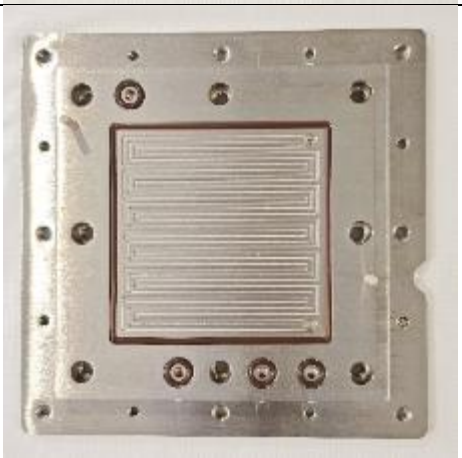
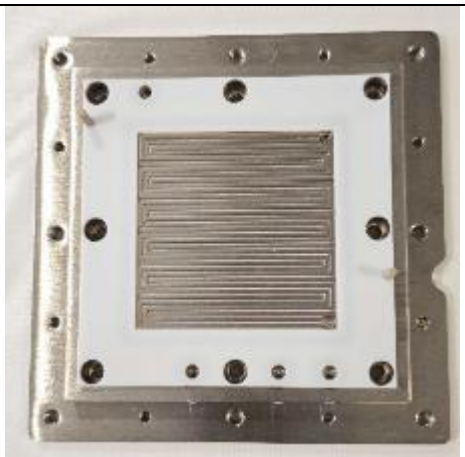
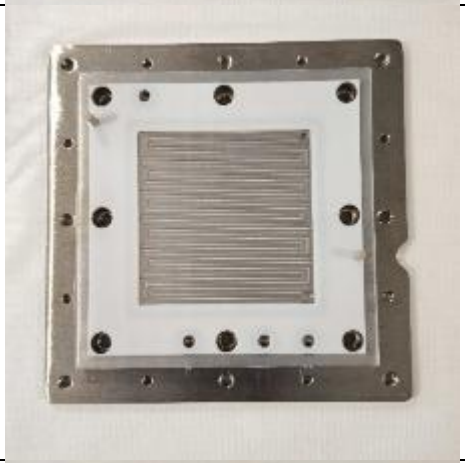
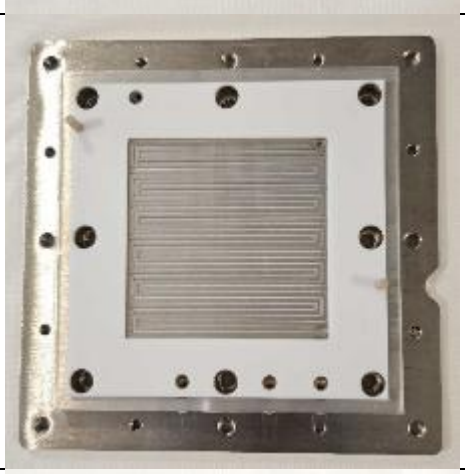


Figure 1. Exploded view of the PHOTOSINT PEC cell (02/2026 design iteration) with component labels.

The following table shows the cell assembly procedure:

1	Position the heat exchanger plate as shown in the photo. Prepare two rectangular O-rings and two PEEK alignment pins.	
2	Screw the two PEEK alignment pins into the holes in the heat exchanger plate. Fit the two O-rings into the grooves shown in the photo.	

3	Fit the O-rings to the front compartment flow field as shown in the photos. Install two rectangular O-rings on the side facing the heat exchanger and five O-rings in total on the side with the flow channels.	 
4	Carefully place the PEEK flow field onto the front compartment flow field, aligning the holes for the alignment pins.	
5	Carefully hold the front compartment flow field and the PEEK flow field together. Place them onto the heat exchanger plate, using the alignment pins to position both parts.	

6	Place one PTFE gasket on the front compartment flow field, as shown in the photo.		
7	Place the GDL coated with a water-splitting catalyst (not shown here) into the opening in the PTFE gasket. Then place the ion-exchange membrane or diaphragm on top, as shown in the photo.		
8	Place the second PTFE gasket over the membrane or diaphragm, as shown in the photo. The opening in the 2nd PTFE gasket is to be filled with a GDL coated with the catalyst for the cathodic process, either CO_2 reduction (CO_2RR) or hydrogen evolution (HER).		
9	Fit all five O-rings into the grooves in the rear compartment flow field, as shown in the photo.		

10	Carefully place the rear compartment flow field onto the cell assembly. If the O-rings slip out of their grooves, use a thin PTFE film to hold them in place while carefully lowering the rear compartment flow field onto the alignment pins.	
11	Insert all eight screws and tighten them by hand until finger-tight.	
12	Using a torque wrench, tighten each screw to 15 lbf·in in a star (crosswise) pattern, as shown in the photo.	
13	Repeat the same star (crosswise) tightening sequence, increasing the torque to 30 lbf·in for each screw.	
14	Repeat the same star (crosswise) tightening sequence, increasing the torque to 45 lbf·in for each screw.	

Table 1 Cell assembly

Since the cells are already assembled and mounted in the panels, steps 1–6 can potentially be omitted. The cell can instead be opened carefully by removing only the rear-compartment flow-field plate. This remains possible despite the Fresnel lenses already being installed, provided that a small supporting frame is used, for example, a flat metal bar supported by two wooden blocks.

2.2.2 Electrolyte circulation and gas management

Peristaltic pumps were selected as the principal circulation technology because of their tolerance to gas-liquid mixtures, flexibility in accommodating different hydraulic configurations, including cells connected in parallel or in series, and ease of integration. The two electrode compartments were designed to use independent reservoirs and circulation circuits, primarily to avoid product crossover. In particular, oxygen generated at the anode should not be allowed to reach the cathode because oxygen reduction could compete with the intended hydrogen evolution or CO_2 reduction reactions and decrease Faradaic efficiency. The reservoirs were also intended to function as gas-liquid separators in a closed-loop electrolyte circulation system. Gas-tight containers with limited headspace were preferred in order to limit ingress of atmospheric oxygen

- For Pilot #1, the proposed hydraulic arrangement consists of three parallel lines, each comprising three cells connected in series. As outlined in D3.3, the cathode was to be supplied with humidified gaseous CO_2 rather than a circulating liquid catholyte. Initially, pure bottled CO_2 was foreseen, followed later by operation using the Torrecid industrial CO_2-containing stream, which was expected to contain approximately 6% oxygen. The industrial stream would be compressed and stored in an intermediate tank. An inlet pressure of approximately 1-2 bar was considered sufficient to provide the required flow through the system, eliminating the need for a separate CO_2 pump downstream of the storage system. Before entering the electrochemical cells, CO_2 was to pass through a bubbler for humidification. However, as described in the Adaptations Introduced During Pilot Construction section, the cathode-feed concept of Pilot #1 was subsequently modified, and the final configuration uses a gas–liquid mixture of DI water and CO_2.

For Pilot #2, the system was configured as four parallel lines, each comprising four cells connected in series. For the hydrogen pilot, operation with 1 M KOH at temperatures up to approximately 60°C was considered. Borosilicate bottles were proposed because of their availability, transparency, and acceptable chemical resistance. Thermal insulation and relatively small electrolyte volumes were preferred because part of the system concept relied on utilization of the heat generated by the PV modules to increase the electrolyte temperature

2.3 Light concentration, thermal integration and tracking

The optical concept retained the use of 15 × 15 cm Fresnel lenses with a focal length of 16 cm. Each electrochemical/PV unit was equipped with its own lens, maintaining the one-cell/one-PV-module/one-concentrator concept. The lens mounting allowed adjustment of the distance between approximately 6 and 9 cm. Experimental work indicated improved concentration efficiency at approximately 8 cm compared with 6 cm, although the longer working distance also increased sensitivity to the angle of incident light.

Because the Fresnel system showed strong angular sensitivity, a commercial dual-axis solar tracker was incorporated into the pilot design. The tracker continuously adjusted

panel orientation based on a light sensor and two actuators. The selected system had a maximum supported mass of approximately 90 kg, 1500 N actuators consuming around 8 W, and a maximum system height below approximately 1.8 m. An 8 Ah $LiFePO_4$ battery was proposed for autonomous tracker operation, while a wind sensor provided automatic movement toward a safer horizontal position during excessive wind.

The multicell panels were designed around 3-mm stainless-steel supporting plates measuring approximately 45 × 45 cm for Pilot #1 and 60 × 60 cm for Pilot #2, reinforced using 20 × 20 mm aluminum profiles. Approximately 5 cm of clearance behind the main plate was reserved for hydraulic tubing and electrical wiring.

2.4 Temperature and electrical monitoring

Temperature monitoring was planned at both the PV module and electrochemical-cell level. Within the EC cell, only the anodic compartment was selected for temperature measurement because the two compartments were assumed to operate close to thermal equilibrium and the anodic side contained liquid electrolyte in both pilots. Because of the geometrically symmetrical panel arrangements, continuous measurement of every cell was considered unnecessary. Four representative cells were selected on each panel, with two measurements per cell, PV temperature and anodic-compartment temperature, resulting in eight temperature channels per pilot. Pt100 sensors and a Digilent 8-channel temperature data logger were selected.

The same principle of representative monitoring was adopted for electrical measurements. Rather than instrumenting every electrochemical cell, the design proposed monitoring two representative complete strings and two representative individual cells. Both voltage and current were measured for these four electrical units, requiring eight differential measurement channels. The data will be collected with a multichannel DAQ unit (DAQ), configured to track 4 voltage and 4 current channels.

Voltage dividers were required because the PV voltage could exceed the ±10 V input range of the DAQ, particularly during concentrated illumination. Current measurement was to be performed indirectly from the voltage drop across 0.5 Ω shunt resistors. The electrical measurements were also intended to enable estimation of Faradaic efficiency by integrating current over time and comparing the resulting total charge with the measured amount of reaction product.

2.5 Expected product generation and product monitoring

For Pilot #1, the initial system calculations assumed a current of 240 mA and a 40% Faradaic efficiency toward methanol. Under these assumptions, the estimated methanol production was approximately 0.024 mL h^{-1} per cell, or approximately 0.22 mL h^{-1} for the complete nine-cell panel, corresponding to about 22 mL during 100 hours of operation. Because of this low production rate, direct liquid-flow measurement was considered impractical and gravimetric collection using a precision balance was proposed.

For Pilot #2, calculations assumed approximately 320 mA per cell/string and 95% Faradaic efficiency for hydrogen evolution. The resulting expected dry hydrogen production was approximately 139 mL h^{-1} per cell, corresponding to roughly 37 mL min^{-1} for the 16-cell panel. A differential-pressure flow meter was selected following comparison with a thermal flow sensor. The hydrogen stream would be separated from the circulating electrolyte in the catholyte reservoir, dried using silica gel or calcium

chloride, and subsequently measured. Periodic samples could additionally be collected for gas-chromatographic analysis, while the remaining small hydrogen flow could be vented safely rather than being utilized industrially.

2.6 Photovoltaic modules and catalyst integration

The original CSIC-developed perovskite modules demonstrated suitable photovoltaic performance, including a 9 × 9 cm 4S4P architecture, but insufficient long-term operational stability became an important integration risk. Encapsulated Solaronix perovskite modules were therefore identified as the most practical alternative for pilot operation. Although they offered somewhat lower efficiency and current density than the CSIC modules, their substantially improved stability over periods of weeks or months was considered more important for pilot-scale testing. Their higher voltage and lower current output also directly motivated the parallel-PV/series-EC electrical architecture described above.

For the electrochemical subsystem, the methanol cathode was based on a (CoPc+Mg^{2+})(2)/CNT catalyst deposited on a gas-diffusion electrode, with a Sustainion membrane and PTFE sealing components. Laboratory CO_2-reduction tests described in D3.3 used 0.5 M $KHCO_3$ anolyte, CO_2 flows around 50 mL·min^{-1} and current densities in the 50-200 mA cm^{-2} range as results of task1.3

For oxygen evolution, mixed-metal oxide catalysts supported on nickel foam were developed, with Zirfon UTP 220 selected as the separator for alkaline water electrolysis. Large-area electrodes were designed around the 49 cm^2 active area required for pilot integration, with preparation of 16 electrodes for the hydrogen pilot. The HER electrode developed by NIC in task 1.4 was based on a Mo-$MnFe_2O_4$-derived catalyst grown on nickel foam, also intended for production of at least 16 equivalent electrodes for multicell integration.

2.7 Adaptations Introduced During Pilot Construction

Although Deliverable D3.3 outlined the principal system components and their integration into the complete pilot assemblies in a comprehensive manner, several minor modifications were introduced during the subsequent construction of the pilots. These changes did not alter the general system architecture established in D3.3, but were implemented to improve energy efficiency, reproduce operating conditions established during Task 2.5, and strengthen system monitoring as result of task 3.2 and 3.3

The need for the first modifications became apparent shortly after delivery of the larger production batch of PEC cell components. In particular, the PEEK insulating liners used around the cell bolts, which prevent electrical short-circuiting caused by direct contact between the bolts and the conductive cell plates, did not fit correctly into the corresponding openings. At approximately the same time, feedback received from SU within Task 2.6 indicated the need to increase the compression of the carbon paper forming the cathode-side gas diffusion layer. The final solution therefore consisted of replacing the original bolts with a different bolt configuration, in which the bolt head remains outside the rear plate of the cell. Electrical insulation is provided by a PEEK washer positioned on top of a stainless-steel washer, while an additional heat-shrink sleeve is applied to the upper section of the bolt to further reduce the risk of electrical contact between the bolt and the conductive cell components, as shown in Figure 2.



Figure 2. Final bolt-insulation solution implemented in the PEC cells. A PEEK washer and heat-shrink sleeve provide electrical insulation from the conductive cell components.

Regarding the need for increased compression of the cathodic gas diffusion layer, tests performed using pressure-sensitive paper showed that insufficient compression occurred mainly in the central region of the cell plate, furthest from the perimeter bolts. This was not considered critical for the PEC cells used in Pilot #2 for hydrogen evolution, where both electrodes have an area of 7 × 7 cm and are based on highly conductive nickel foam. However, the issue is considerably more important for Pilot #1, where the cathode area was ultimately reduced to approximately 5 cm² and positioned in the center of the plate. In this configuration, adequate compression of the central region is essential to ensure reliable electrical contact. For this reason, the spacing between the ion-exchange membrane and the cathodic flow field was required to remain below approximately 0.25 mm.

To improve compression in this region, custom pressure springs were designed and manufactured, as shown in Figure 3. The springs are fabricated from a stainless-steel grade suitable for elastic spring applications and formed into a U-shaped geometry, with the central section applying additional force to the middle of the cell plate. Tests using pressure-sensitive paper confirmed that this solution significantly improved pressure distribution in the central region. As an additional measure, the thickness of the PTFE gasket on the cathodic side of the Pilot #1 cells was reduced from 0.25 mm to 0.20 mm, further improving compression and electrical contact at the cathode.

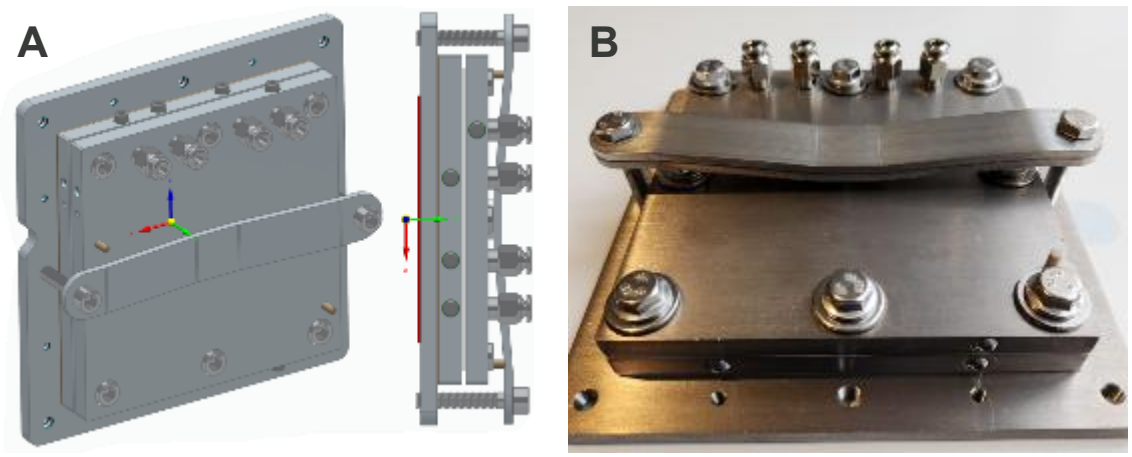


Figure 3. PEC cell for methanol production in Pilot #1 equipped with the additional pressure spring. (A) 3D models of the modified cell assembly. (B) Photograph of the assembled cell. Based on the compression tests, the preferred configuration uses two stacked leaf springs with a moderate degree of bending.

Further modifications were introduced during the actual assembly of the pilots. First, the electrolyte circulation system was revised. The Peristaltic Pump Model A (Redox.me) originally selected in D3.3 was replaced by a dual-channel peristaltic pump BT600L (Lead Fluid). D3.3 considered separate pumping of the anodic and cathodic circuits using the selected single-channel pump. The use of a dual-channel pump makes it possible to operate both circuits using a single pumping unit, reducing the overall energy

consumption of the system. This solution is applicable because the same electrolyte flow rate is required on the anodic and cathodic sides of the hydrogen pilot. When identical peristaltic tubing is installed in both pump channels, both circuits are therefore operated at the same flow rate. In addition, the new pump provides a maximum flow rate of up to 1200 $mL \cdot min^{-1}$, removing the previously considered limitation of approximately 95 $mL \cdot min^{-1}$ per hydraulic line. Consequently, Pilot #2 can reproduce the conditions used during the experiments performed within Task 2.5, where a flow rate of 100 $mL \cdot min^{-1}$ per cell was applied. The pilot consists of four parallel hydraulic lines, each containing four cells connected in series. A flow rate of 100 $mL \cdot min^{-1}$ will therefore be applied through each line of Pilot #2, corresponding to a total flow of 400 $mL \cdot min^{-1}$ on both the anodic and cathodic sides.

Nextmodification, concerns the cathode feed of Pilot #1. In D3.3, the cathodic compartment was planned to be supplied with humidified gaseous CO_2. In the final pilot configuration, the cathodic side is instead supplied with DI water combined with a gaseous CO_2 stream immediately before the panel inlet using a Y-shaped connector. A check valve is installed in the CO_2 line to prevent water from entering the gas-supply line. This configuration provides the water required for the CO_2 reduction reaction while maintaining a gas-liquid feed that limits the risk of excessive flooding of the cathodic compartment. The total flow rates supplied to each individual cell in Pilot #1 are 10 $mL \cdot min^{-1}$ of DI water and 50 $mL \cdot min^{-1}$ of CO_2. No changes were introduced on the anodic side. As specified in D3.3, the anolyte consists of 0.5 M $KHCO_3$ and is supplied at a flow rate of 10 $mL \cdot min^{-1}$ to each individual cell.

An additional advantage of this configuration is that the produced methanol is expected to accumulate predominantly in the liquid catholyte, facilitating its collection compared with recovery directly from a gaseous outlet stream. At the end of the experiment, methanol can be separated from water by conventional distillation, taking advantage of the difference between their boiling points. Since the catholyte receives heat transferred from the photovoltaic modules and consequently operates at elevated temperature, some methanol may nevertheless leave the system with the outlet gas. To reduce these losses, the gas leaving the cathodic compartment will be directed through an additional container filled with DI water and maintained at ambient temperature. This container will act as a secondary methanol trap. Following completion of the planned 100 h experiment, the contents of both collection vessels will be combined for subsequent product recovery and analysis.

The third modification concerns the voltage and current monitoring strategy. D3.3 proposed monitoring selected representative strings and individual cells, based on the geometrical symmetry of the panels and the expected similarity between equivalent positions. During construction, it was decided instead to prioritize monitoring of all complete electrical strings, consisting of parallel-connected PV modules supplying series-connected electrochemical cells. This approach reduces the risk that underperformance or failure of a PV module or electrochemical cell within an unmonitored string remains undetected. Measurements will be performed using the same multichannel DAQ described in D3.3, configured for four voltage and four current measurement channels.

For Pilot #2, the four available voltage and current channels will therefore be used to monitor all four strings. In Pilot #1, only three strings are present, leaving one voltage and one current channel available for component-level monitoring. The monitored component can be selected during pilot operation and changed periodically, for example between a corner cell and the central cell of the 3 × 3 panel. Considering the electrical architecture of the system, the additional voltage channel will be used to monitor an individual electrochemical cell, whereas the additional current channel will be used to

monitor an individual PV module. This provides complementary information, since cells connected in series carry the same string current, while the current contribution of individual PV modules connected in parallel may differ.

Finally, the last minor change concerns the default flow distribution configuration of Pilot #1. The initial design considered three parallel hydraulic lines, each comprising three cells connected in series. However, post-assembly testing (described in a separate section below) showed that, at the relatively low flow rates used in Pilot #1, the distribution of liquid between the parallel branches was not sufficiently uniform. This is most likely related to the low hydraulic resistance of the individual flow paths and the resulting small pressure drop, under which even minor differences in tubing geometry, connections, or manifold flow paths can lead to noticeable differences between the branch flow rates. For operation at the Torrecid site, the default flow path was therefore rearranged into a fully serial configuration, eliminating the need for flow splitting and ensuring that the same gas-liquid stream passes through each of the nine cells. This modification is fully compatible with the flexible hydraulic concept envisioned in the project proposal, according to which the pilot flow distribution can be readily reconfigured between fully parallel and fully serial arrangements. The original 3 × 3 configuration can therefore be restored if required. In such a case, backpressure regulators or needle valves can be installed at the outlets of the three parallel lines to balance their hydraulic resistance and improve the uniformity of the flow distribution.

2.8 Post-Assembly Validation and Functional Testing

Following completion of the assembly of both pilots, a series of validation tests was performed to verify the correct operation of the individual components and of the integrated systems. Particular attention was given to confirming mechanical stability, leak tightness, correct operation of the monitoring equipment, and proper hydraulic performance. These tests were also intended to minimize the risk of damage to the surrounding equipment caused by mechanical failure, such as loosening or detachment of components, or by chemical exposure resulting from electrolyte leakage.

i) Solar tracking system

After installation of the supporting frame and all electrochemical cells, the solar tracking system was tested under the full mechanical load of the assembled panel. The purpose of this test was to confirm that the actuators remained capable of moving the complete assembly throughout their full operating range. Test runs performed for both pilots confirmed that the additional mass of the assembled panels did not interfere with normal tracker operation. This was particularly relevant for Pilot #2, where the total load exceeded 50 kg. The observed performance was consistent with the manufacturer's specification, which states a maximum supported load of 90 kg.

ii) Leak testing of the electrochemical cells and assembled panels

Leak tightness was evaluated both at the level of the individual electrochemical cells and after their integration into the complete panel. Each cell was initially tested for approximately 30 min at a water flow rate of 800 $mL \cdot min^{-1}$. This value is considerably higher than the flow rates anticipated during normal pilot operation, which are typically in the range of approximately 10-100 $mL \cdot min^{-1}$ per hydraulic line. The elevated flow rate was intentionally applied to test the sealing performance under increased hydraulic pressure, exceeding 2 bar. Such conditions provide a conservative test of the cell integrity. Although the nominal hydraulic configuration of Pilot #2 consists of four parallel lines, each containing four cells connected in series, one of the project assumptions is

that the hydraulic connections may be rearranged depending on the operating requirements, ranging from a fully parallel to a fully serial configuration. The elevated-flow test therefore verifies that the cells remain leak-tight even under the most demanding hydraulic arrangement, in which all cells are connected in series, and the cells located at the beginning of the line are exposed to the highest pressure.

Following assembly of the complete panels, extended leak tests were performed continuously for more than 100 h. For approximately half of this period, water was circulated at 57-60 °C. This test reproduced conditions representative of pilot operation with heat transferred from the photovoltaic modules to the circulating electrolyte. It also provided testing under reduced liquid viscosity associated with elevated temperature. No leakage was observed during either the individual-cell or complete-panel tests.

iii) Temperature and electrical data-acquisition systems.

The monitoring systems were tested prior to pilot operation to verify correct sensor operation, channel configuration, and data acquisition. The temperature-logging system was evaluated using the actual temperature sensors installed in the pilots. The voltage and current DAQ system were tested using a Solaronix photovoltaic module together with resistive loads in the range of approximately 20-50 Ω. The different resistances were used to simulate variations in the electrical load presented by the electrochemical cells, which depend on the electrochemical reaction, operating temperature, and pilot configuration. These tests confirmed correct acquisition and recording of the electrical signals over the relevant operating range.

iv) Hydrogen flow measurement

For Pilot #2, the differential-pressure hydrogen flow meter was independently tested before integration into the final system. The test confirmed that the factory calibration of the instrument provided correct flow readings within the operating range relevant to the pilot and that no additional calibration adjustment was required before deployment.

v) Uniformity of flow distribution between hydraulic lines

The hydraulic design of both pilots was initially based on manifolds dividing the flow delivered by the pump between several parallel hydraulic lines. Pilot #1 contains three parallel lines, while Pilot #2 contains four. Although the systems were designed to be geometrically symmetrical, the actual flow distribution between the individual branches was experimentally verified after assembly.

As a result of this test, the hydraulic configuration of Pilot #1 prepared for operation at the Torrecid site was changed from three parallel lines to a fully serial arrangement. As described in the *Adaptations Introduced During Pilot Construction* section, in this configuration, the DI water stream is mixed with CO_2 immediately before the panel inlet using a Y-shaped connector, after which the gas-liquid mixture passes consecutively through all nine cells. The applied flow rates are 10 $mL \cdot min^{-1}$ for DI water and 50 $mL \cdot min^{-1}$ for CO_2.

For Pilot #2, where the target flow rate is 100 $mL \cdot min^{-1}$ per line, the flow distribution between the four parallel branches was found to be sufficiently uniform. In contrast, for Pilot #1, operated at substantially lower liquid flow rates, significant differences between the individual branches were observed. This behaviour is most likely related to the very low hydraulic resistance of the individual lines and, consequently, the small pressure drop generated at these flow rates. Under such conditions, even minor differences in

tubing geometry, connections, or manifold flow paths can result in noticeable differences in the flow distributed between parallel branches.

vi) Additional functional checks

Several additional checks were performed on auxiliary components, including verification of the electrical resistance and continuity of the installed cables and confirmation of the correct operation of the PC units used for system control and data collection. All validation tests were completed successfully, with no significant issues identified. The results confirmed both the appropriate selection of the system components and their correct integration into the assembled pilot systems

2.9 Operational conditions for pilots

Although most of the operational conditions for the two pilots have already been described they are summarized here for clarity and ease of reference. The main operating parameters for both pilots are collected in Table 2.

Table 2. Operational conditions

Parameter	Pilot #1 - MeOH	Pilot #2 - Hydrogen
Catholyte composition	DI water and CO_2 gas	1M KOH
Catholyte flow	10 and 50 ml/min	100 ml/min
Anolyte composition	0.5 M $KHCO_3$	1M KOH
Anolyte flow	10 ml/min	100 ml/min
Volume of catholyte and anolyte per reservoir	300 - 350 ml	400 - 450 ml
Default flow distribution configuration	9 cells connected in series	4 parallel lines, each comprising 4 cells connected in series
PTFE gasket for cathodic flow field	0.20 mm thick, with 2.24 x 2.24 cm opening	0.8 mm thick, with 7 x 7 cm opening
PTFE gasket for anodic flow field	0.8 mm thick, with 7 x 7 cm opening	

The volume of catholyte and anolyte given in Table 2 should be treated as an initial range and verified experimentally during pilot start-up, as the exact volume cannot be determined reliably before the cells are loaded with the final electrode assemblies. After the panel and tubing are fully filled, approximately 100–150 mL of electrolyte should remain in each reservoir. Such electrolyte volume should be sufficient to prevent the pump from running dry. At the same time, enough free space should be maintained in the reservoir to accommodate electrolyte that may drain back from the panel and tubing by gravity if the pump is disconnected, thereby preventing leakage outside the system.

For Pilot #2, the hydrogen stream directed to the flow meter is dried using $CaCl_2$ granules. Both drying tubes should be filled with the drying agent before operation. The $CaCl_2$ will require periodic replacement; however, the appropriate replacement interval cannot be defined in advance, as the amount of water vapor carried by the hydrogen stream depends on the electrolyte temperature, which in turn is influenced by the ambient temperature and the amount of heat transferred from the photovoltaic modules. The drying tubes should therefore be inspected after each day of operation. Since the two tubes are connected in series, the first tube is expected to become saturated more rapidly and will likely require more frequent replacement.

For both cell types, the assembly bolts are tightened in three successive torque steps of 15, 30, and 45 lb·in. For Pilot #1, the bolts used to compress the leaf spring should be tightened gradually until the threaded end of each bolt is level with the outer surface of the heat-exchanger flow-field plate. The default settings of the solar trackers have not been modified and should be adjusted according to the conditions at the deployment site, particularly the light-intensity threshold used to trigger actuator movement.

2.10 Equipment images

2.10.1 Pilot 1 Methanol production

Due to the operating principle of the solar tracking system, the pilot panel must be installed with a defined orientation relative to the cardinal directions. For this reason, the descriptions of the photographs refer to the corresponding north, south, east, and west directions when indicating the viewing angle and tracker position.



Figure 4. Photographs of Pilot #1 showing the assembled panel from different viewing angles and tracker positions. (A, C) Panel with the cell-supporting frame in its western most position, viewed from the east and west sides, respectively. (B, D) Panel with the cell-supporting frame in its easternmost position, viewed from the east and west sides, respectively.

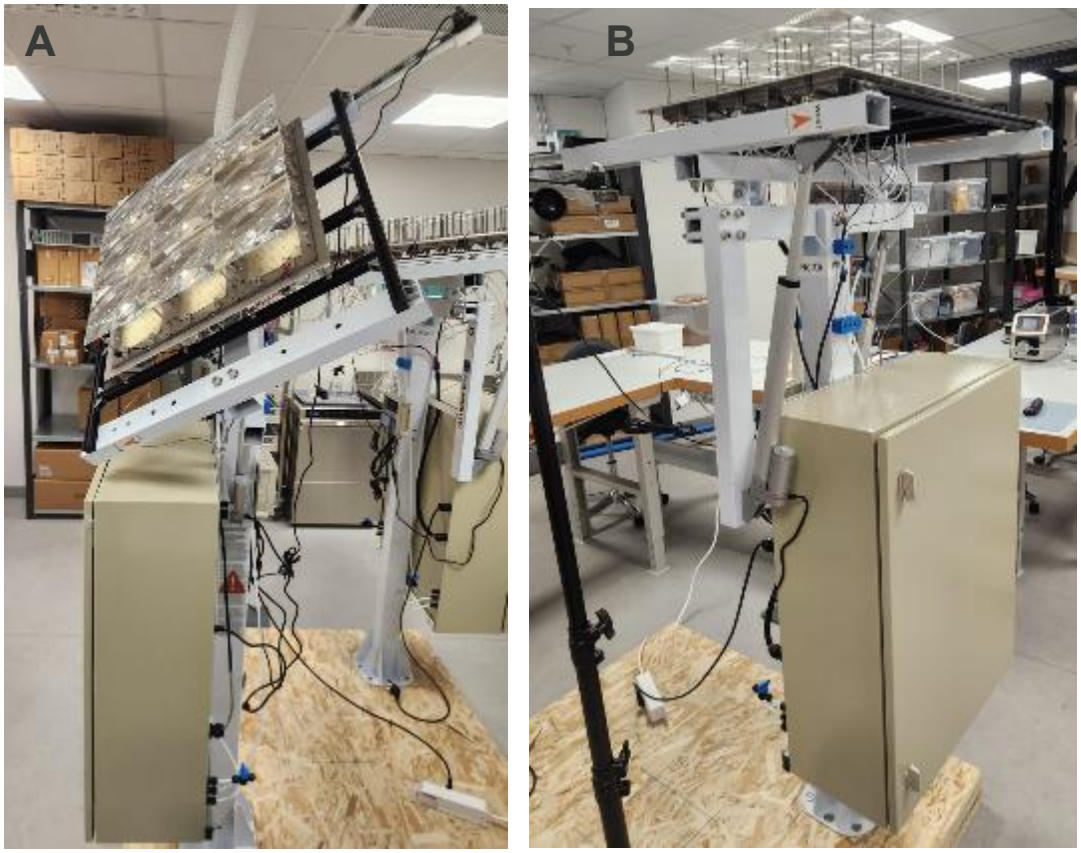


Figure 5. Photographs of Pilot #1 viewed from the south and north sides. (A) South-side view with the cell-supporting frame in its southeastern most position. (B) North-side view with the cell-supporting frame in the fully horizontal position.

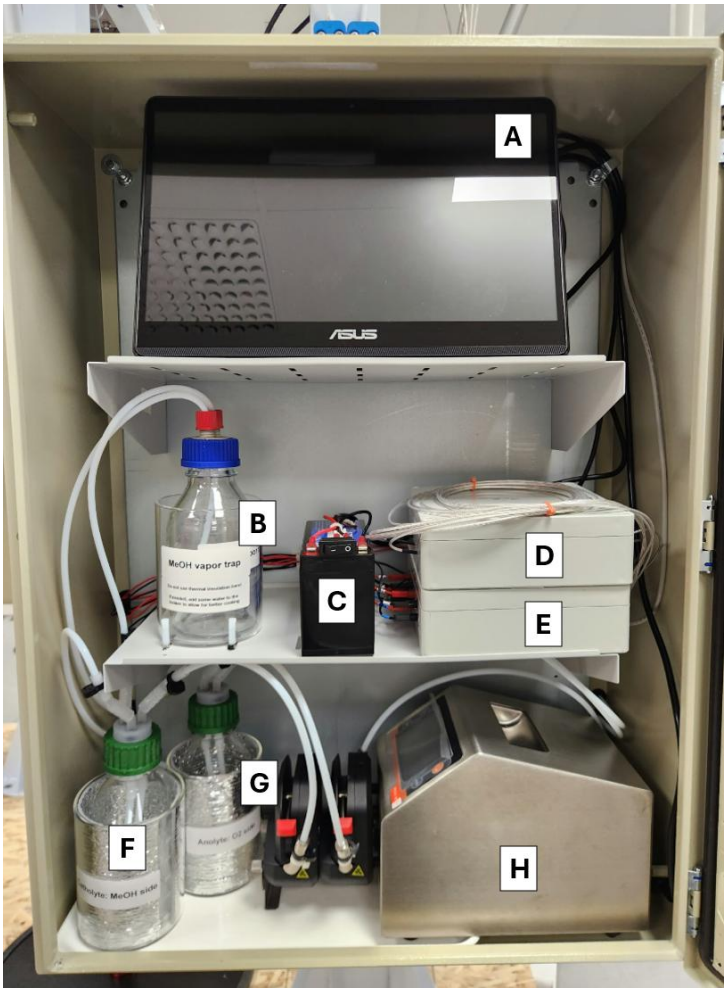


Figure 6. Internal components of the electrical enclosure of Pilot #1. (A) PC running Windows OS, used for data acquisition and data storage. (B) Secondary methanol vapour trap: DI-water-filled container maintained at ambient temperature. (C) LiFePO4 battery (8 Ah) supplying power to the solar tracking system. (D) Temperature data logger: electrical enclosure housing the Digilent USB-TEMP device, to which the Pt100 temperature sensors are connected. (E) Current and voltage data logger: electrical enclosure housing the Digilent USB-1608GX-2AO DAQ device together with resistors and capacitors used for signal conditioning and reliable data acquisition. As described in D3.3, current is measured indirectly from the voltage drop across a shunt resistor using Ohm's law. (F) Catholyte reservoir, also serving as a collection vessel for methanol (in aqueous solution) and as a gas–liquid separator for the CO_2 stream leaving the panel. (G) Anolyte reservoir, also serving as a gas-liquid separator for the oxygen stream. The separated oxygen is neither dried nor quantified and is instead directed outside the enclosure and released to the atmosphere. (H) Dual-channel BT600L peristaltic pump, used for simultaneous circulation of the catholyte and anolyte.

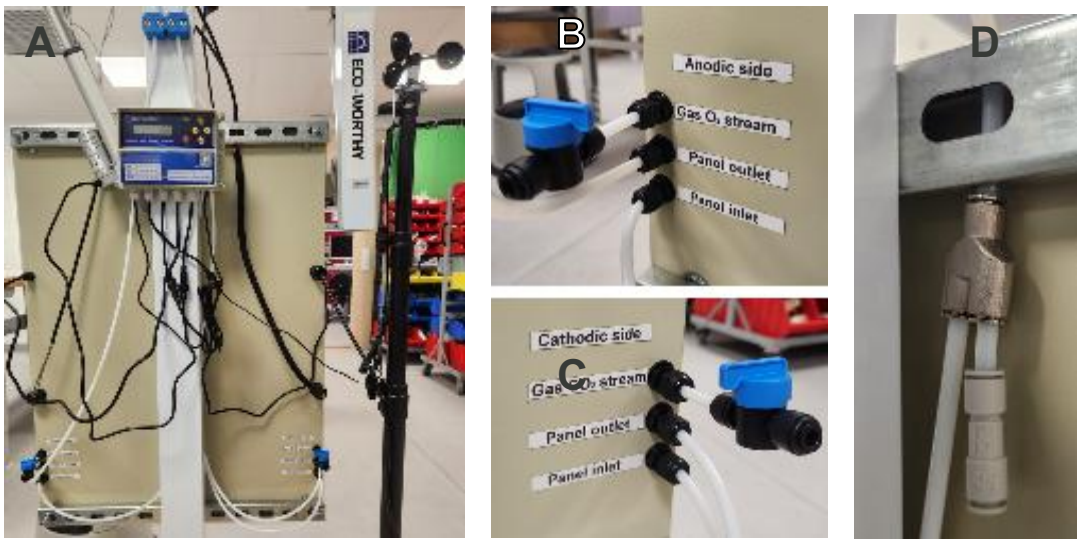


Figure 7. Rear view of the electrical enclosure and associated external components. (A) Overall view showing the rear of the enclosure, including the solar tracker controller mounted on the main tracker pole and the external pole supporting the wind sensor on the right-hand side. (B, C) Close-up views of the tubing connections through the electrical enclosure for the anodic and cathodic sides, respectively. The gas-carrying lines are terminated with on/off valves. All openings introduced by RDM in the electrical enclosure for pilot integration, as well as the electrical connections in the solar tracker wiring as supplied by the manufacturer, are fitted with IP68-rated cable glands to maintain protection against water and dust ingress. (D) Close-up view of the Y-shaped connector used to combine the CO_2 and DI water streams immediately before the cathodic panel inlet. The CO_2 inlet line is equipped with a check valve to prevent water from entering the gas line. The resulting gas–liquid mixture subsequently passes through all nine cells connected hydraulically in series.

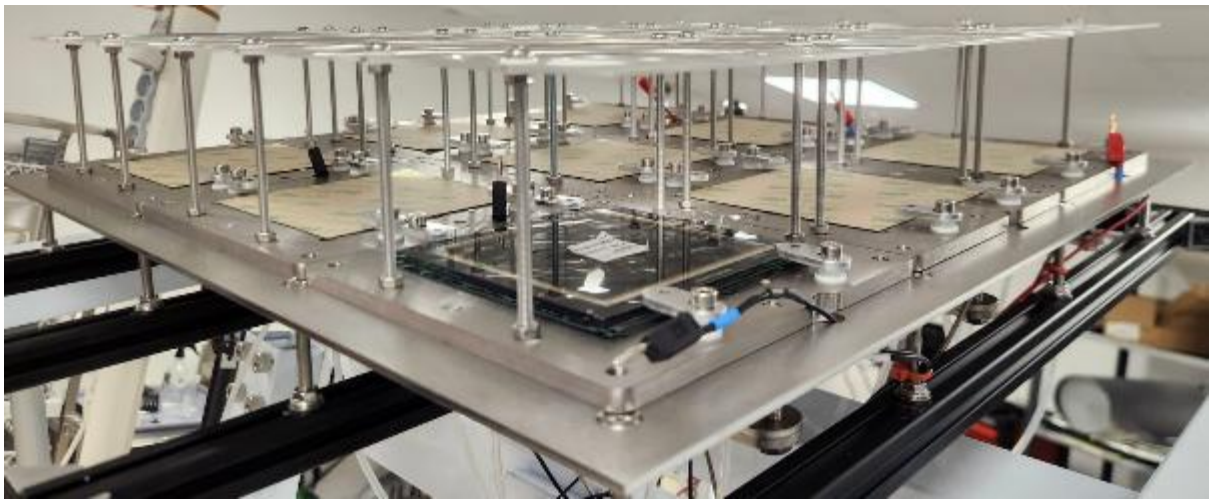


Figure 8. Light concentrators and photovoltaic module mounting arrangement in Pilot #1. Side view of the cell-supporting frame showing the positions for the PV modules and Fresnel lens concentrators. One Solaronix PV module, previously used in stability testing, is installed on the bottom corner cell for demonstration purposes.

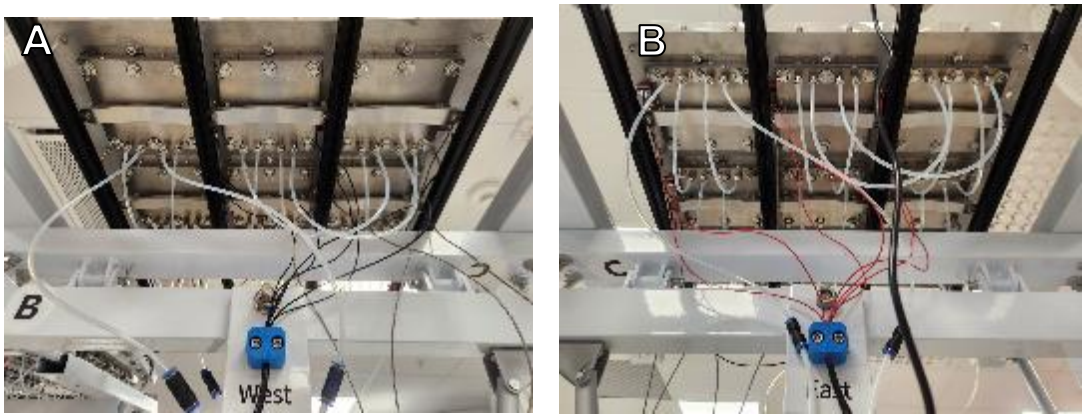


Figure 9. Electrical wiring and hydraulic tubing of the cells with the panel in the horizontal position. (A) View from the west-facing side, showing the panel inlet tubing and the negative (−) electrical connections for both the electrochemical cells and PV modules. (B) View from the east-facing side, showing the panel outlet tubing and the positive (+) electrical connections for both the electrochemical cells and PV modules.

2.10.2 Pilot 2 Hydrogen production



Figure 10. Photographs of Pilot #2 showing the assembled panel from different viewing angles and tracker positions. (A, C) Panel with the cell-supporting frame in its westernmost position, viewed from the east and west sides, respectively. (B, D) Panel with the cell-supporting frame in its easternmost position, viewed from the east and west sides, respectively.



Figure 11. Photographs of Pilot #2 viewed from the south and north sides. (A) South-side view with the cell-supporting frame in its southeasternmost position. (B) North-side view with the cell-supporting frame in the fully horizontal position.

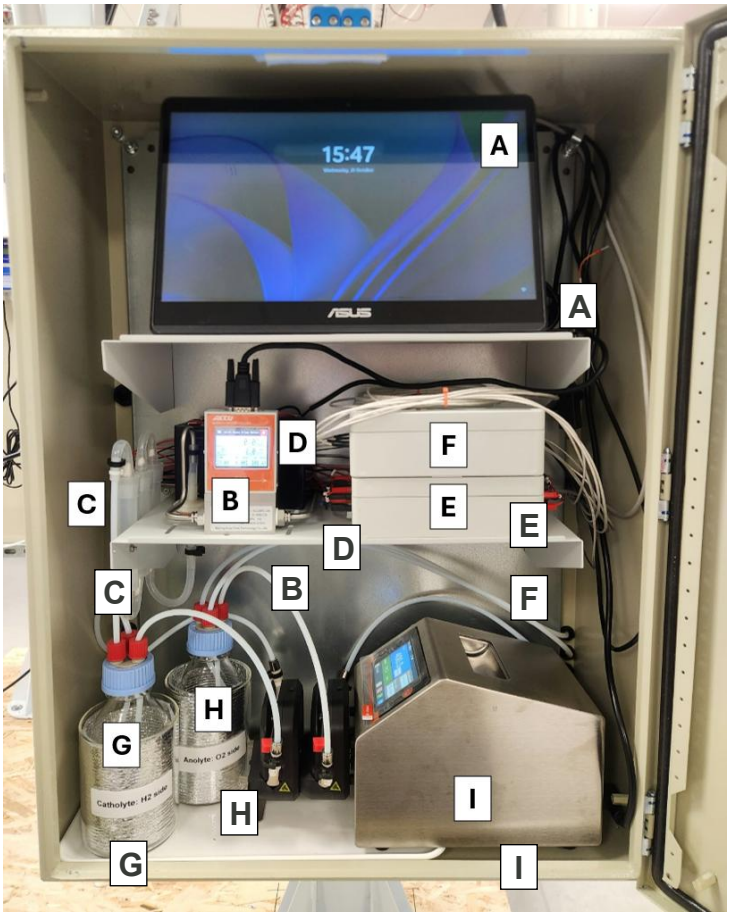


Figure 12. Internal components of the electrical enclosure of Pilot #2. (A) PC running Windows OS, used for data acquisition and data storage. (B) Hydrogen flow meter (ACI30FC), based on a differential-pressure sensor. (C) Drying tubes for removal of water vapour from the hydrogen stream. The tubes are to be filled with anhydrous $CaCl_2$ granules shortly before the start of pilot operation. (D) $LiFePO_4$ battery (8 Ah) supplying power to the solar tracking system. (E) Current and voltage data logger: electrical enclosure housing the Digilent USB-1608GX-2AO DAQ device together with resistors and capacitors used for signal conditioning and reliable data acquisition. As described in D3.3, current is measured indirectly from the voltage drop across a shunt resistor using Ohm's law. (F) Temperature data logger: electrical enclosure housing the Digilent USB-TEMP device, to which the Pt100 temperature sensors are connected. (G) Catholyte reservoir, also serving as a gas-liquid separator for the hydrogen stream. The separated hydrogen is directed through the drying tubes and subsequently to the hydrogen flow meter. (H) Anolyte reservoir, also serving as a gas-liquid separator for the oxygen stream. The separated oxygen is neither dried nor quantified and is instead directed outside the enclosure and released to the atmosphere. (I) Dual-channel BT600L peristaltic pump, used for simultaneous circulation of the catholyte and anolyte.



Figure 13. Rear view of the electrical enclosure and associated external components. (A) Overall view showing the rear of the enclosure, including the solar tracker controller mounted on the main tracker pole and the external pole supporting the wind sensor on the left-hand side. (B, C) Close-up views of the tubing connections through the electrical enclosure for the anodic and cathodic sides, respectively. The gas-carrying lines are terminated with on/off valves. All openings introduced by RDM in the electrical enclosure for pilot integration, as well as the electrical connections in the solar tracker wiring as supplied by the manufacturer, are fitted with IP68-rated cable glands to maintain protection against water and dust ingress.



Figure 14. Light concentrators and photovoltaic module mounting arrangement in Pilot #2. (A) Side view of the cell-supporting frame showing the mounting positions for the PV modules and Fresnel lens concentrators. (B) Close-up view of a cell with the PV module installed, together with the negative-side wiring prepared for parallel connection of the negative terminals of all PV modules within the corresponding line. (C) Close-up view of a cell before installation of the PV module. The thermal interface sheet is visible on the heat exchanger surface and is used to improve heat transfer between the PV module and the heat exchanger.

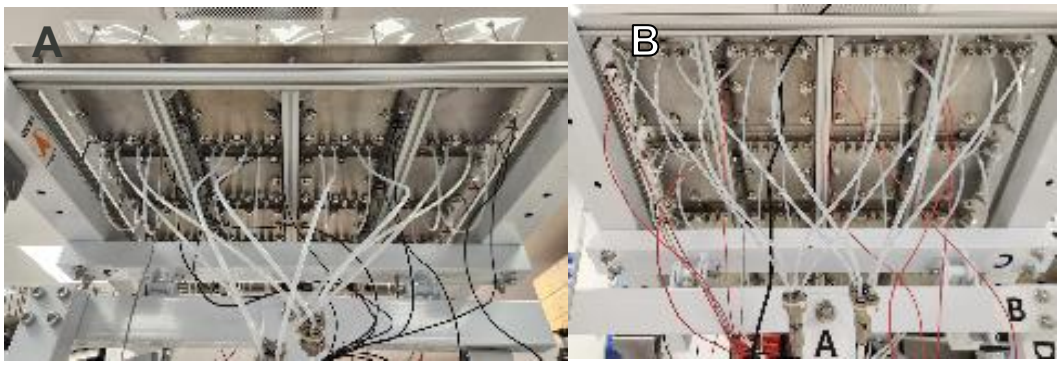


Figure 15. Electrical wiring and hydraulic tubing of the cells with the panel in the horizontal position. (A) View from the west-facing side, showing the panel inlet tubing and the negative (−) electrical connections for both the electrochemical cells and PV modules. (B) View from the east-facing side, showing the panel outlet tubing and the positive (+) electrical connections for both the electrochemical cells and PV modules. Light concentrators and photovoltaic module mounting arrangement in Pilot #2. (A) Side view of the cell-supporting frame showing the mounting positions for the PV modules and Fresnel lens.

2.11 Health and safety guidelines and regulations

In terms of STE and TOR, both pilots have to fulfil specific health and safety rules. Specifically, H&S rules applying at TOR are:

Table 3 H&S standards at TOR

Standard	Regulation
Real Decreto 1644/2008	Regulations on equipment installation
Real Decreto 1215/1997	Regulations on workers' safety by use of equipment
Real Decreto 485/1997	Regulations on safety and risk assessment
Real Decreto 773/1997	Regulations on the use of PPE
Real Decreto 486/1997	Regulations on safety environment
Real Decreto 614/2001	Regulations against electric risks
Real Decreto 842/2002	Regulations on low voltage installations
Real Decreto 100/2011	Regulation on gas emissions to the atmosphere
2006/42/EC	Machinery Directive
2004/108/EC	Electromagnetic Compatibility
EN ISO 12100:2010	Safety of machinery - General principles for design - Risk assessment and risk reduction
EN 60204-1	Safety of machinery – Electrical equipment of machines

In the case of Steklarna Hrastnik, PHOTOSINT pilot #2 remains well below every regulatory threshold that would trigger formal hydrogen permitting. Nevertheless, even a 2 L/h electrolyser can accumulate flammable or explosive gas mixtures, and its oxygen by-product poses a hazard in its own right. Consequently, under the Slovenian Regulations on Explosion Protection (Official Gazette of the RS No. 41/16), any use of explosive gas requires a documented explosion and hazardous-area risk assessment of the project — that is, an Explosion Hazard Study. A Fire Safety Study must also be carried out. The regulations to be followed for the project are listed in Table 4 Additional regulations and standards will be applied in preparing the studies.

Table 4 Slovenian legislation to be respected for the PHOTOSINT piloting activities

LIST OF NATIONAL REGULATIONS CONCERNING SAFETY ISSUES	
(Official Gazette of the RS No 41/16	Regulations on explosion protection
Official Gazette of the RS No 89/99, 39/05	Regulation on requirements for ensuring the safety and health of workers at workplaces
Official Gazette of the Republic of Slovenia No 3/07. 9/11, 83/12, 61/17 – GZ, 189/20 – ZFRO and 43/22.	Fire Protection Act
Official Gazette of the RS No 12/13	Regulation on the design and study of fire safety

At the time of preparing this deliverable, the studies are not yet completed. Depending on the results of these studies, for example, in case of identification of ATEX zones, mitigation measures will need to be applied, and the final configuration of the pilot may differ from the present one.

3. INTEGRATION OF PILOTS AT DEMO

3.1 Integration of methanol pilot at Torrecid

The pilot will be integrated at the Torrecid plant. The plant is located in Alcora, Castellón. PHOTOSINT will implement the pilot plant close to the furnace.



Figure 16 View of TOR plant

For industrial supply of CO_2, a pipe must be connected to the furnace; a 20 cm diameter pipe has been considered initially. In terms of material, temperature and corrosion, AISI 310 has been selected, as well as a small fan. The process takes the fumes from a gas-O_2 furnace to have a higher CO_2 concentration.

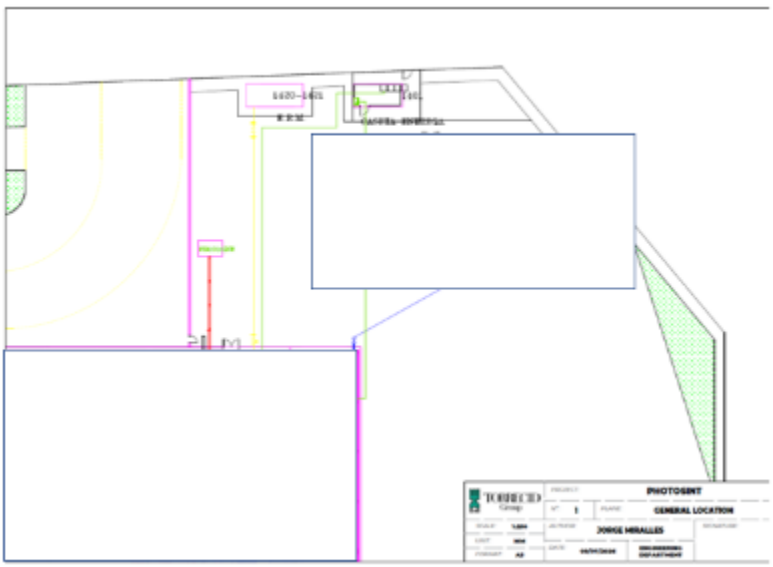


Figure 17 Implementation in TOR plant

, The following auxiliaries have been defined :

i) Water: Osmotized water, pH 7.5, conductivity 100 mS, amount needed 0.6 ml/h, which will be supplied by TOR.

ii) Electrolyte (supported by system).

iii) Electrical power for auxiliary systems: 200 W; connection will be supplied by TOR.

iv) CO_2 supply 1 bar 0.016 m^3/h. The pilot plant will be fed in preliminary tests with pure CO_2 before testing industrial CO_2. Will be supplied by TOR.

v) Waste disposal: the main waste comes from the electrolyte. The methanol-producing electrocatalyst has a limited lifetime and therefore will have to be replaced every 100-200 h of operation. Also, even despite using DI water for preparation of the electrolyte, there will be a need to replace it every few hundred hours, meaning that there will be a small volume of 0.5 L per week of $KHCO_3$ water solution. Waste material will be sent for authorized disposal by TOR.

3.2 Integration of Hydrogen pilot at Steklarna

Pilot #2 for hydrogen production will be installed at Steklarna Hrastnik on one of the flat roofs, to enable appropriate illumination of the pilot. The final choice will be made according to the findings of the Explosion hazard study and Fire safety study.

The operation of the pilot #2 does not require a permanent water supply connection. During routine operation activities, the system will be supplied from a 10 L reservoir containing deionized water (and purified wastewater for the second stage of testing), which is sufficient for the anticipated hydrogen production rates and testing activities.

Due to the low hydrogen production rate, the hydrogen generated by Pilot #2 will not be supplied to the industrial nor pilot glass melting furnace at Steklarna Hrastnik. Consequently, no hydrogen transfer pipelines or process integration infrastructure are required between the pilot installation and the furnace. All hydrogen produced during the demonstration activities will be used exclusively for performance characterization and purity assessment.

4. CONCLUSION

This deliverable presents the pilot lines assembly and systems that will be integrated at the demo. The document provides an overview of assembled pilots, including photovoltaics, cells, electrolyte, monitoring system and validation tests performed, including explanation on specific assembly parts. In addition, an overview of location at demo site and implementation regulations have been reported. Deliverable 3.4 is key for validation since it also provides operating conditions of both pilots.